International Journal of Mechanical, Industrial and Aerospace Sciences
ISSN: 2517-9950
Vol:10, No:8, 2016

Balancing and Synchronization Control of a Two Wheel Inverted Pendulum Vehicle

Shiuh-Jer Huang, Shin-Ham Lee, Sheam-Chyun Lin

Abstract**—**A two wheel inverted pendulum (TWIP) vehicle is built with two hub DC motors for motion control evaluation. Arduino Nano micro-processor is chosen as the control kernel for this electric test plant. Accelerometer and gyroscope sensors are built in to measure the tilt angle and angular velocity of the inverted pendulum vehicle. Since the TWIP has significantly hub motor dead zone and nonlinear system dynamics characteristics, the vehicle system is difficult to control by traditional model based controller. The intelligent model-free fuzzy sliding mode controller (FSMC) was employed as the main control algorithm. Then, intelligent controllers are designed for TWIP balance control, and two wheels synchronization control purposes.

Keywords**—**Balance control, synchronization control, two wheel inverted pendulum, TWIP.

I. INTRODUCTION

TWO wheels mobile platform and humanoid mobile robot are interesting application of inverted pendulum system. Various nonlinear control algorithms were proposed to monitor inverted pendulum dynamic response behavior [1]-[3] by taking care of the highly nonlinear time varying dynamics. After the control strategy development of inverted pendulum stabilization and balancing are matured, the two wheels inverted vehicle system was designed as the short distance mobile tool. Ha and Yuta [2] designed a TWIP and proposed a balancing and trajectory tracking controller. Grasser et al. [3] designed a JOE system and derived its dynamic model based Newton's method. Then, two wheels input torque are decoupled into two subsystems for balancing and steering control purposes. Pathak et al. [4] employed model-based partial feedback linearization method to manipulate vehicle moving speed and position. Chiu and Peng [5] proposed a two control loops scheme with inner loop for balancing control and outer loop for position control. Ren et al. [6] proposed a self-tuning PID controller for vehicle motion speed monitoring with velocity feedback signal to convert into inclining angle for balancing. Ding and Cheng [7] designed and evaluated their performances of double PID control and LQR control. The well known TWIP vehicle is Segway designed by Dean Kamen [8] with 5 gyroscope and two inclination sensors to derive vehicle information for motion control. General motor and Segway cooperated to design a two person electric vehicle PUMA with 56km/hr maximum speed and 56km distance of travel for each electric charge.

Since, most of previous studies are focused on the inverted pendulum balancing and moving control without precise quantitative moving speed and parking position motoring capability; here, a prototype TWIP vehicle is built with two hub motor and embedded gyroscope and accelerometer sensors. The model-free intelligent FSMC was designed to monitor the vehicle balancing, and synchronization control.

II. COMPONENTS OF TWIP VEHICLE

The main frame of this TWIP vehicle was made of stainless tube to support one-person weight as Fig. 1. It has a handle bar to adjust the moving speed. For the balancing and motion control purposes, 3 axes accelerometer sensor MMA7361 is chosen to measure the gravity direction for deriving inclination angle, 2 axes gyroscope LPY503AL was built to measure the angular velocity. The inclination angle estimated from accelerometer is:

$$\theta \approx \frac{V_y - V_{basic} - \ddot{x}_{motor}}{V_z - V_{basic}} \tag{1}$$

where V_{basic} , V_y and V_z are accelerometer analog output voltage at 0g, current y and z directions, respectively. $\ddot{x}_{motor}$ is the vehicle moving acceleration derived from two hub motors angular position variation based on encoder feedback. The rotational velocity components (rad/sec) of vehicle come from gyroscope are:

$$\omega_x \approx 0.0017(V_x - V_{ref}),\ \ \omega_z \approx 0.0017(V_z - V_{ref}) \tag{2}$$

where V_x , V_{ref} and V_z are gyroscope analog output voltage measurement values.

In order to record the vehicle motion information and update the MCU control program, Zbee S1 wireless communication module was selected to connect the MCU and PC with UART transmission interface. For simplifying the transmission structure of this vehicle, low cost 300 W permanent magnet DC brushless hub motor is chosen for each wheel. The tire outside diameter and periphery are 12.5 inch and 1 m, respectively. Since, this hub motor has not position encoder, an encoder is installed with belt system connection to feedback the rotation angle. The resolution is 12000 counts per circle. This hub motor has obviously driving deadzone due to embedded reducing gear mechanism. The no-load motor rotation speed with respect to

Shin-Ham Lee, Sheam-Chyun Lin are with the National Taiwan University of Science and Technology, Taipei, 106, Taiwan (e-mail: m10203408@ mail.ntust.edu.tw, sclynn@mail.ntust.edu.tw).

Shiuh-Jer Huang is with the National Taiwan University of Science and Technology, Taipei, 106, Taiwan (Corresponding author, phone: 886-2-27376449; fax: 886-2- 27376460; e-mail: sjhuang@mail.ntust.edu.tw).

the input voltage is shown in Fig. 2. It has about 5V deadzone control voltage. The TWIP vehicle deadzone control voltage is even large than 9V. It will cause a harsh control problem.

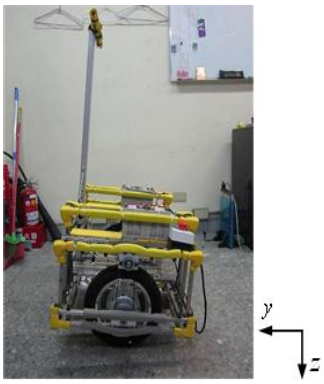

Fig. 1 TWIP vehicle side view

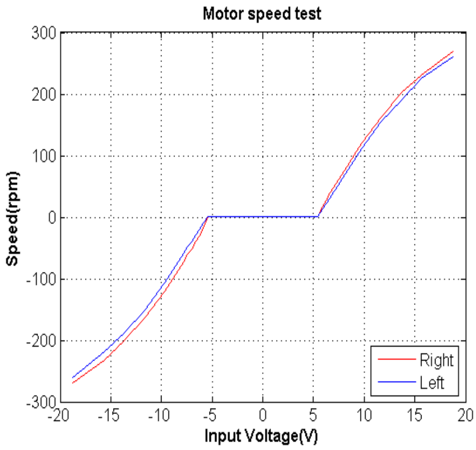

Fig. 2 Hub motor no-load dead zone

ARduino Nano ATMEGA328P-AU microprocessor was chosen as the control kernel of this TWIP vehicle. It has embedded flash memory to store control program and data, UART and I2C communication port. The wireless communication module was chosen to transfer the vehicle motion situation to outboard PC for analysis purpose without addition cable line. ATMEGA328 has two 8bits timer counter equipped with PWM output and overflow interrupt and one 16bits counter register. Here timer2 overflow interrupt is set as fixed system control frequency 100 Hz. Timer1 generates 25 KHz high frequency PWM signal. This microprocessor also has 8 channel ADC for converting the sensors' analog feedback signals into digital for MCU control purpose. ATMEGA318 provides a 8bits external interrupt port for pin change interrupt (PCINT) function. Here, Port B and post D signals change interrupt are used to read in two wheels rotational encoder signals. When encoder's A or B phase have change, the PCINT is excited to read in signal for judging the rotation direction and position counter value add or subtract. The overall TWIP vehicle system control board is shown in Fig. 3. The analog signal is connected with a first order Rc low pass filter to suppress the noise.

III. TWIP Vehicle Driving Control

Since the TWIP wheel inverted pendulum vehicle system has time-varying and complicate driving control dynamics, it is difficult to establish an accurate dynamics model for model based controller design. Here, the model free intelligent FSMC scheme is employed as the kernel control strategy to design the balancing, and two wheels synchronous control laws for this TWIP vehicle. The brief derivation of this FSMC control law and each sub system control law are described in following sections.

A. FSMC Control Algorithm

A sliding surface on the phase plane is defined as

$$s(t) = (\frac{d}{dt} + \lambda)e_1 = e_2 + \lambda e_1 \tag{3}$$

where $e_i = x_{id} - x_i$ are defined as the state control errors. The sliding variable, s, will be used as the input signal for establishing a fuzzy logic control system to approximate the specified perfect control law, u_{eq}. With this perfect control law, the closed loop control system has an asymptotical stability dynamic behavior.

$$\dot{s}(t) + \lambda s(t) = 0 \tag{4}$$

Since λ is a positive value, the sliding surface variable, s, will gradually converge to zero. Based on the definition of sliding surface variable, s, in (4), the system output error will converge to zero, too. In this study, a fuzzy system is employed to approximate the mapping between the sliding variable, s, and the control law, u, instead of model-based calculation. This control law may have certain difference with the perfect control law u_{eq}, and then the following equation can be derived:

$$\dot{s}(t) = -\lambda s(t) + b(X,t)[u_{eq}(t) - u(t)] \tag{5}$$

Generally, $b(X)$ is a positive constant or a positive slow time-varying function for practical physical systems. By multiplying both sides of the above equation with s gives

$$s(t)\dot{s}(t) = s(t)\{-\lambda s(t) + b(X,t)[u_{eq}(t) - u(t)]\} \tag{6}$$

Based on the Lyapunov theorem, the sliding surface reaching condition is $s \cdot \dot{s} < 0$. If a control input u can be chosen to satisfy this reaching condition, the control system will converge to origin of the phase plane. It can also be found that $\dot{s}$ increases as u decreases and vice versa in (6) If $s > 0$, then the increasing of u will result in $s\dot{s}$ decreasing. When the condition is $s < 0$, $s\dot{s}$ will decrease with the decreasing of u. based on this qualitative analysis, the control input u can be designed in an attempt to satisfy the inequality $s \cdot \dot{s} < 0$. The relating theory about the convergence and stability of the adaptation process based on the minimization of $s\dot{s}$ can be found in [9].

Here, a fuzzy logic control is employed to approximate the nonlinear function of equivalent control law, u_{eq}. The control voltage change for each sampling step is derived from fuzzy inference and defuzzification calculation instead of the equivalent control law derived from the nominal model at the sliding surface. It can eliminate the chattering phenomenon of a traditional sliding mode control. The controller design does not need a mathematical model and without constant gain limitation. The system control block diagram is shown in Fig. 4. The one dimensional fuzzy rules is designed based on the sliding surface reaching condition, $s \cdot \dot{s} < 0$. The sliding surface variable, s, is employed as the one dimensional fuzzy input variable. Here, the input and output membership functions are scaled into eleven subsets within the range of -1 and +1 with equal span. Hence a scaling factor gs is employed to map the sliding surface variable, s, into this universe of discourse. A scaling factor gu is employed to adjust the value of control voltage.

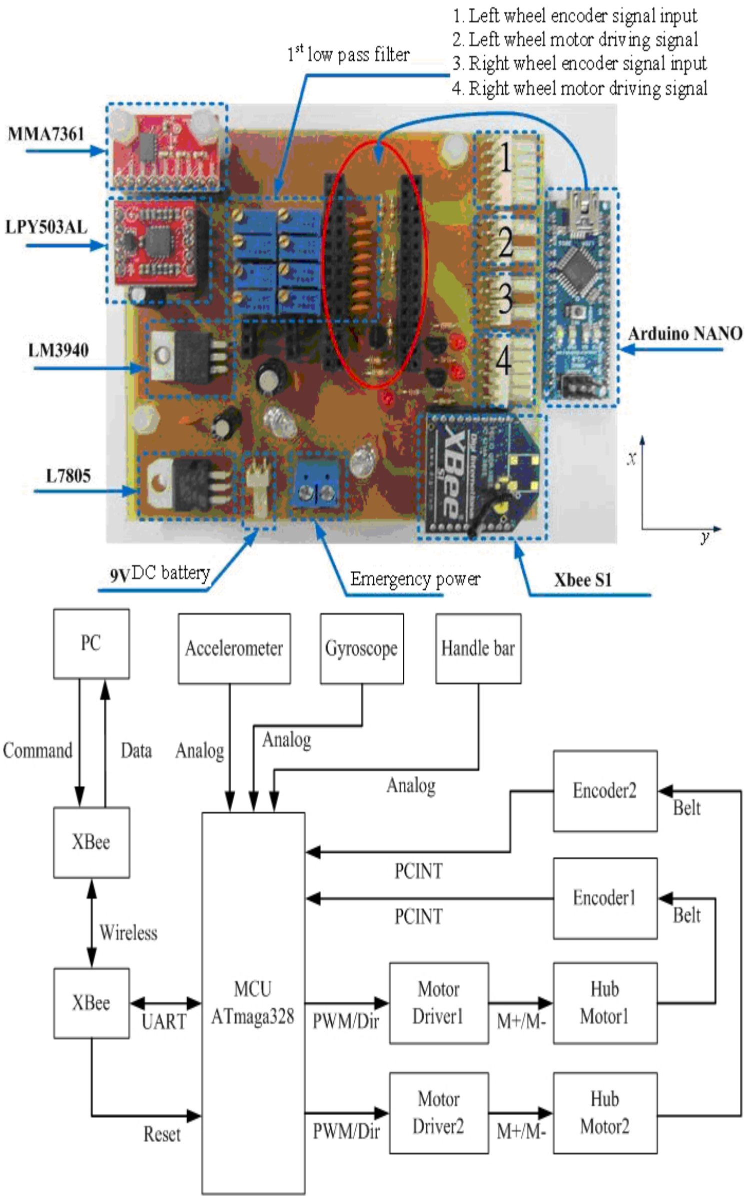

Fig. 3 TWIP vehicle control board picture and mechatronics system block diagram

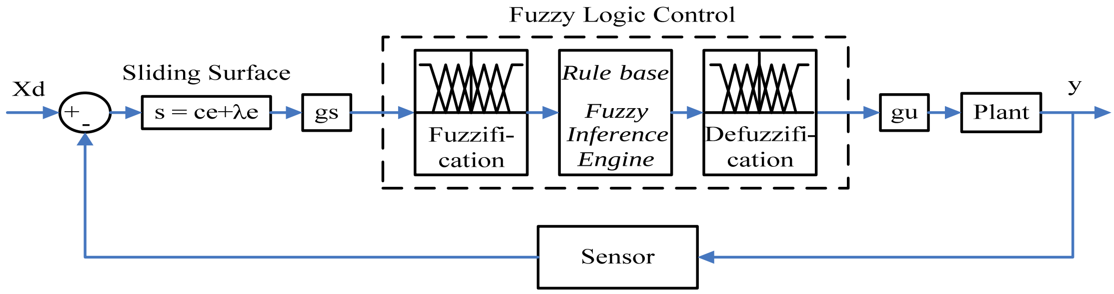

Fig. 4 FSMC block diagram

The membership function used in this paper for the fuzzification is of a triangular type. The function can be expressed as

$$\mu(x) = \frac{1}{w}(-|x-a| + w) \tag{7}$$

where w is the distribution span of the membership function, x is the fuzzy input variable and a is the parameter corresponding to the value 1 of the membership function. The height method is employed to defuzzify the fuzzy output variable for obtaining the PWM control duty cycle of the wheel motor driver. Which is a nonlinear function derived from the fuzzy inference decision and defuzzification operation.

$$u = \frac{\sum_{l}^{m} \mu^{j} \cdot U^{j}}{\sum_{l}^{m} \mu^{j}} = \frac{\sum_{l}^{m} \mu^{j} \cdot C^{j}}{\sum_{l}^{m} \mu^{j}} \equiv \sum_{1}^{m} \phi_{j} C^{j} \tag{8}$$

where m is the rules number and C^j is the consequent parameter. Here, eleven equal-span triangular membership functions are used for the fuzzy input variable, s, and output variable, u.

B. Vehicle Balancing Control

Since the stable balancing is the most basic requirement for a TWIP vehicle, the balancing control strategy was designed. The balancing controller is designed based on FSMC scheme. If the vehicle posture is forward leaned, the vehicle should move forward for maintaining stable up-right position. Conversely, vehicle should move backward to overcome vehicle leaning back. Then, the FSMC balance controller is designed with inclination angular error and angular speed error as input signals to obtain the control input PWM duty cycle for both hub motors. Since, this TWIP vehicle has significantly deadzone motor control voltage between 8.7 ~ 9.3V, it should be considered during control law calculation. The traditional handling method is to add on the deadzone value into the calculated control law. However, it will cause high frequency control voltage chattering and driving circuit problems when the vehicle reaches the up right position ($\theta = 0^{\circ}$). Here, the motor deadzone behavior is embedded designed in the fuzzy control rules subset to eliminate this characteristic. The balancing controller control block diagram and control parameters are shown in Fig. 5.

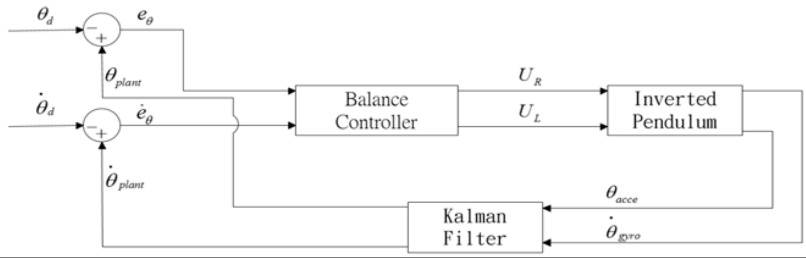

fuzzy control input variables	$s = \lambda e + \dot{e}$, $e_\theta = \theta - \theta_d$, $\dot{e}_\theta = \dot{\theta} - \dot{\theta}_d$
gs	450
gu	480
fuzzy membership function S	[-1.0 -0.55 -0.35 -0.25 -0.03 0 0.03 0.25 0.35 0.55 1.0]
fuzzy membership function U	[-1.0 -0.9 -0.85 -0.65 -0.5 0 0.5 0.65 0.85 0.9 1.0]

Fig. 5 Balancing controller control block diagram and control parameters

C. Two Wheels Synchronous Control

Since, two hub motors motion were monitored with individual controller and driving circuit, they will have obviously wheel speed difference due to mechanism and electric components variation. If it was not compensated, that will induce vehicle motion path deviation, especially obvious in long distance travelling. Hence, a two wheels synchronous controller should be designed for future vehicle motion path or parking position control. Here, the FSMC controller is designed with two wheels position error e_{p-diff} and velocity error $\dot{e}_{p-diff}$ as input signals to obtain the control input PWM duty cycle for left hub motor compensation value. The system control block diagram and the control parameters are listed in Fig. 6. Where P_{w-d} and V_{w-d} are two wheels differential objectives. They should be set as zero for two wheels synchronous control without speed difference.

IV. Experimental Results

Here, the model free intelligent FSMC scheme is employed as the kernel control strategy to design the balancing, and two wheels synchronous control laws for this TWIP vehicle. The closed loop sampling frequency is set as 100 Hz. The vehicle motion dynamics information were transmitted to PC through XBee wireless communication module with 20 Hz frequency. The PC record data includes vehicle inclination angular velocity (mrad/sec) of gyroscope, vehicle inclination angle (mrad), motor encoder and change rate and motor PWM control signal. Those signal were converted into vehicle inclination angle (degree), angular velocity (degree/s), moving distance (m) and velocity (m/sec) and hob motor control voltage (V) by MATLAB tool box for figures plotting and analysis.

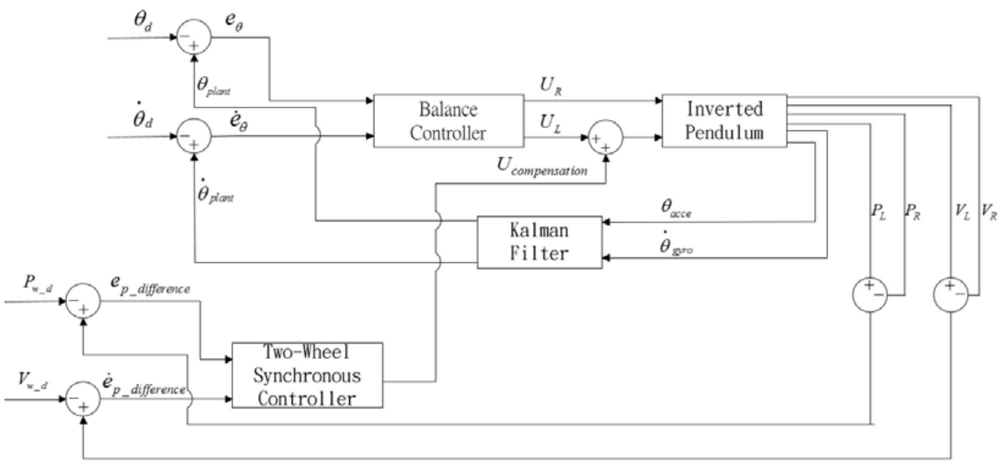

fuzzy control input variables	$s=\lambda e+\dot{e}$, $e_{p\_difference}=(P_L-P_R)-P_{w\_d}$, $\dot{e}_{p\_difference}=(\dot{P}_L-\dot{P}_R)-\dot{P}_{w\_d}$
gs	200
gu	120
fuzzy membership function S	[-1.0 -0.8 -0.6 -0.4 -0.2 0 0.2 0.4 0.6 0.8 1.0]
fuzzy membership function U	[-1.0 -0.9 -0.7 -0.5 -0.3 0 0.3 0.5 0.7 0.9 1.0]

Fig. 6 Two wheels synchronous control block diagram and control parameters

A. Vehicle Balancing Control

Single control law value is derived from FSMC controller to monitor both hub motor back and forth motion, simultaneously. The FSMC control rules were listed in Fig. 5. The non symmetric triangular membership functions were employed with deadzone values 0.03 and 0.5 for S and input U inner fuzzy set, respectively. The corresponding control voltage for U=0.5 is 9V. When the sliding variable s less than 0.03, the motor control input voltage is within its deadzone and motor is stall. The experimental results of vehicle tilt angle, control voltage and both wheels position response during 40 seconds balancing control are shown in Figs. 7 (a), (b) and (c), respectively. During first 6 seconds, the vehicle lean angle within threshold, the vehicle is stable stall within the deadzone area with motor stop. After that, the vehicle is controlled to move back and forth for maintaining stable up-right with control law larger than 9V deadzone value. The vehicle tilt angle is controlled within in 0.5º. The RMS of vehicle tile angle during 40 seconds control period is 0.112º of this study.

B. Two Wheels Synchronous Control

The FSMC control parameters and fuzzy control rules are listed in Fig. 6. Here, the control purpose is to equalize both wheels motion dynamics. Hence, both wheels differential objectives P_{w-d} and V_{w-d} are set as zero. This control law correction value was added to the left hand side motor. If the vehicle is operated under random handle disturbance 45 seconds without synchronous control inner loop, the both wheels travelling position difference will has 26 cm. It is not acceptable for vehicle path tracking or parking position control purposes. The experimental results of vehicle tilt angle, both wheels travelling velocity and positions, and position difference responses during 45 seconds synchronous control are shown in Figs. 8 (a), (b), (c) and (d), respectively. Both wheels position difference is significantly reduced to 2 cm and both wheels have almost the same speed responses curves.

V. Conclusion

A TWIP vehicle system was constructed with Arduino Nano control kernel and accelerometer gyroscope sensors feedback. The harsh hub motor control voltage deadzone feature was overcome with a skill fuzzy control rules design for significantly eliminating the control law chattering. The intelligent FSMC control strategy was proposed to design the balancing, and two wheels synchronous motion, respectively. The vehicle velocity control error and parking position error are less than 2.8 cm/s and both wheels position difference is significantly reduced to 2 cm, respectively. That means the proposed control structure is a general purpose solution for TWIP vehicle applications.

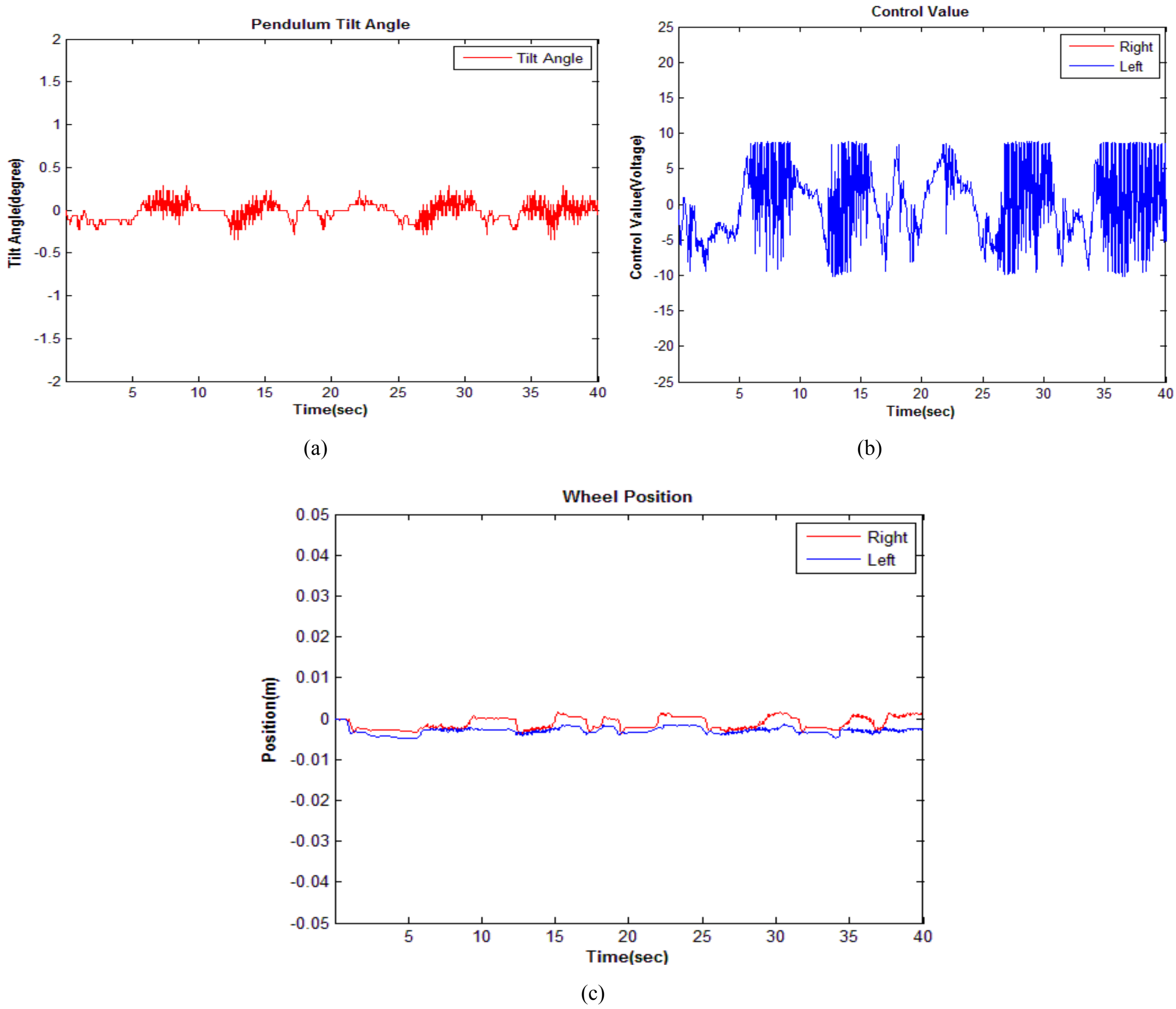

Fig. 7 (a)Vehicle tilt angle, (b) control voltage and (c) both wheels position response during 40 seconds balancing control

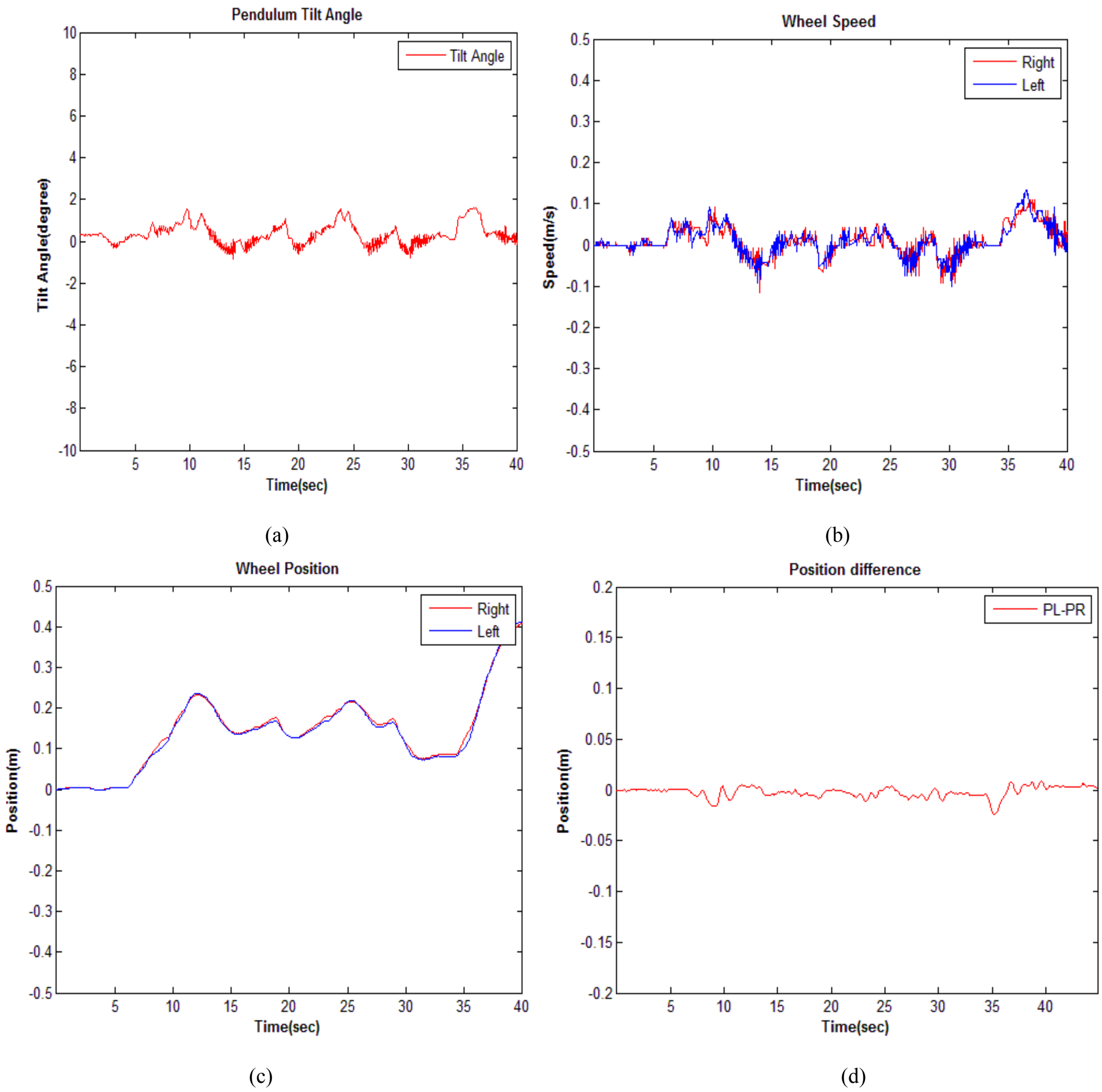

Fig. 8 (a) Vehicle tilt angle, (b) both wheels travelling velocity, (c) positions, and (d) position difference responses during 45 seconds synchronous control

ACKNOWLEDGMENT

The authors would like to thank the financial support of Taiwan National Science Council under the contract NSC-101-2221-E- 011-004-MY3 and Taiwan Ministry of Science and Technology under the contract MOST 104-2221-E011-034-MY2.

REFERENCES

[1] S. Mori, H. Nishihara, and K. Furuta, "Control of unstable mechanical system control of pendulum," Int. J. Control, Vol. 23. No. 5, pp. 673-692, 1976.
[2] Y. Ha, and S. Yuta, "Trajectory Tracking Control for Navigation of Self-Contained Mobile Inverse Pendulum," IEEE/RSJ/GJ Int. Conf Advanced Robotic Systems and the Real World, Munich, Germany, Vol. 3, pp. 12-16, September 1994.
[3] F. Grasser, A. D'Arrigo, S. Colombi, A. C. Rufer, "JOE: a mobile, inverted pendulum," IEEE Transactions on Industrial Electronics, Vol. 49, 2002.
[4] K. Pathak, J. Franch, S.K. Agrawal, "Velocity and position control of a wheeled inverted pendulum by partial feedback linearization," IEEE Transactions on Robotics, Vol. 21, 2005.
[5] C. H. Chiu, and Y. F. Peng, "Design and Implementation of the self-dynamic Controller for Two-Wheel Transporter," IEEE International Conference on Fuzzy Systems, 2006.
[6] T. J. Ren, T. C. Chen, and C. J. Chen, "Motion control for a two-wheeled vehicle using a self-tuning PID controller." Control Engineering Practice, pp. 365-375, 2007.
[7] W. Li, H, Ding, and K, Cheng, "An Investigation on the Design and Performance Assessment of double-PID and LQR Controllers for the Inverted pendulum," UKACC International Conference on Control, Cardiff, United Kingdom, pp.190-196, September 2012.
[8] Segway of West Texas, "i2 Models," Retrieved July 1, 2015, from http://www.segwaytexaswest.com/i2%20Models.htm
[9] Hwang G C and Lin S C, "A stability approach to fuzzy control design for nonlinear systems," Fuzzy Sets Systems, 48, (1992), pp.269-278.

Shiuh-Jer Huang received the B.Sc. and M.Sc. degrees form National Taiwan University, Taipei, Taiwan, in 1978, 1980, and the Ph.D. degree from the University of California, Los Angeles, in 1986, all in mechanical engineering department. In 1986, he joined the faculty of the Department of Mechanical Engineering, National Taiwan University of Science and Technology, Taipei, Taiwan, where he is currently a professor. His research interests are robotic system control and applications, vibration control, Mechatronics, and vehicle active suspension control.

Shin-Ham Lee is a graduate student in Department of Mechanical Engineering, National Taiwan University of Science and Technology, Taipei, Taiwan.

Sheam-Chyun Lin received the Ph. D degree from Oklahoma University in 1987, in mechanical engineering department. Then, he joined the faculty of the Department of Mechanical Engineering, National Taiwan University of Science and Technology, Taipei, Taiwan, where he is currently a professor. His research interests are fluid mechanics and cooling fan design and analysis.